PAPER • OPEN ACCESS

Application of seismic isolation for multi-story buildings in moderate seismicity areas like Vietnam

To cite this article: Van-Tu Nguyen *et al* 2020 *J. Phys.: Conf. Ser.* **1706** 012119

Application of seismic isolation for multi-story buildings in moderate seismicity areas like Vietnam

Van-Tu Nguyen, Ngoc-Quang Vu and Xuan-Dai Nguyen

Institute of Techniques for Special Engineering, Le Quy Don Technical University, Hanoi, Vietnam.

Email: nguyentu@lqdtu.edu.vn

Abstract : Multi-story buildings are important components of urban infrastructures due to their undeniable advantages. However, their structures are characterized by the mass distributed in height and a great slenderness leading to its earthquake vulnerability. Further, their typical structures designed by the conventional method provide low earthquake resistance. The seismic isolation bearings are considered as an effective solution for the structure located in regions of high and moderate seismic activity. The paper presents the procedure to calculate the isolated building structure located in the moderate seismicity areas such as Vietnam. The bilinear hysteretic model is employed to determine the properties of the isolator through the simplified procedure. Three-dimensional model of a typical 11-story building structure is analyzed to evaluate the effect of the isolator on seismic responses of building. The modal analysis and time history analysis are performed using Etabs V17, with the input record taken according to the earthquake ground motion in Hanoi-Vietnam, calculated by the Vietnamese code. The result shows the high effectiveness of isolator on reducing the seismic effect.

1. INTRODUCTION

The damage and losses caused by earthquakes are enormous, especially for the infrastructure systems. The multi-story building is an important component of urban planning and becoming increasingly popular in big cities. However, its structure is vulnerable to the effects of horizontal dynamic loads, especially under strong impacts like earthquakes and may lead to certain damage or entire building. Therefore, essential building structures shall be designed with high vitality to ensure safety during and after major earthquakes.

The first seismic design approach was based on the demand for elastic forces, ensuring that the structural components are dimensioned with sufficient strength level to meet all the effects of loading in an elastic manner. This approach has proved to be economically unsustainable then it was logically abandoned due to the scarcity of earthquakes. In order to increase economic efficiencies of design, many current standards and specifications define the performance-based seismic design, as a structural approach, which allows for certain structural damage rates according to the specified earthquake intensity [1–5]. However, these accepted damages can lead to the loss of structural operation or the need for major repairs of constructions after the earthquake.

Recently, the use of seismic protection devices is becoming increasingly common for constructions in earthquake areas. These advanced technique offers high energy dissipation capacities and/or high values of the ductility [6–12], significantly reducing the impacts of earthquakes on construction structures.

Seismic base isolation (SBI) has been considered an effective technique for the seismic resistant design by providing a special suspension system that isolates the superstructure of the construction from its substructure [8,13–15]. On the other hand, these systems have a high vertical stiffness to ensure the vertical bearing capability and a sufficient horizontal stiffness under the non-seismic lateral impact to maintain the stability of the construction. They have been widely applied as seismic protection for buildings, bridges, and industrial facilities in the strong earthquake regions such as Japan, the U.S, Turkey, New Zealand, etc. [16]

On the other hand, as the building exposed to the earthquake, SBI introduces flexible supports and high dissipation capacities, allowing the building to be decoupled in the horizontal direction from the ground motion. Figure 1 illustrates the principle of SBI's effects on the seismic responses of the structure from the spectrum point of view.

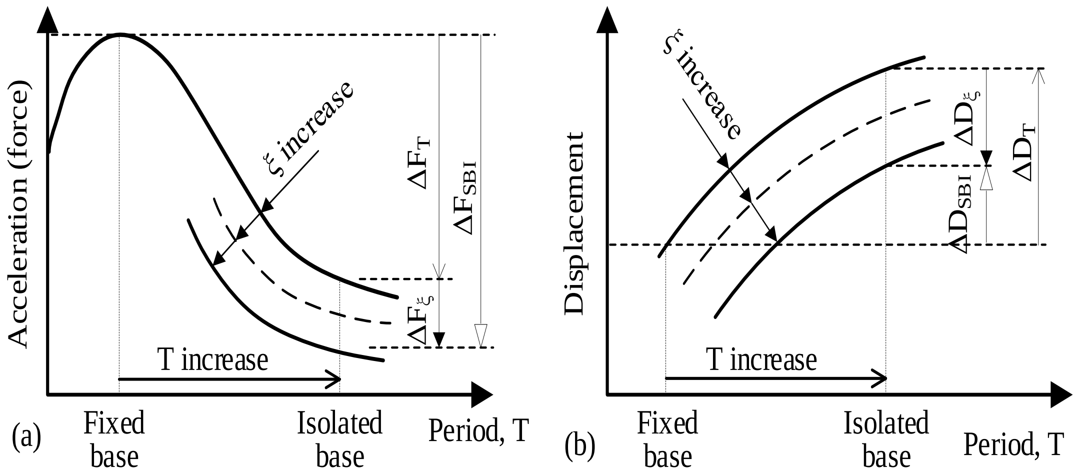

Figure 1. Effects of SBI approach on the seismic responses: (a) on spectral acceleration (lateral force), (b) on lateral displacement.

As observation from the figures, the improvement of structural flexibility by using SBI results in an extension of the fundamental period of vibration leading to a decrease in lateral force and an increase in displacement responses. Added energy dissipation capacity, typically integrated to the SBI, therefore, seems to be the most effective way to reduce the displacement.

A typical application of the SBI device in the global building structure and its behavior under the impact of earthquakes are shown in Figure 2. Accordingly, the isolated building structure includes the superstructure, the isolation, the foundation and soil (i.e. the substructures), order from the top to bottom, respectively. Practically, SBI is considered a connection between the superstructure and the substructure, allowing the building to float on its foundation, resulting in the inconsiderable effect of ground motions and improving earthquake resistances for the building.

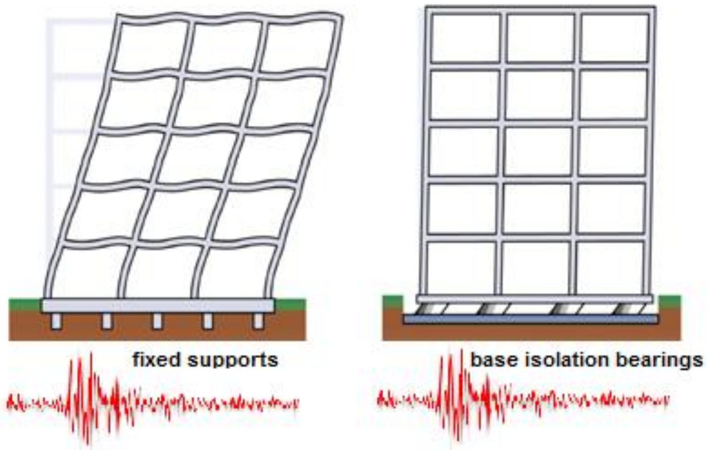

Figure 2. Effects of SBI on contour deformation of the structure.

Generally, seismic isolation technologies fall into two major systems such as elastomer-based and friction-based, categorized according to their respective operating principles. The elastomeric rubber bearings were first used around the 1950s for isolated bridges and then, they have been a very common system of SBI used over many decades based on the high vertical bearing capacity, low horizontal stiffness, and high restoring capability. The most common elastomer-based SBIs are the high damping rubber bearings (HDRB) and lead-plug rubber bearings (LRB). The HDRB uses an elastomer with a special formulation presenting a considerable energy dissipation capacity with an effective damping ratio varying around 10% to 15%. However, it is significantly sensitive by temperature conditions, aging effects, and the scragging phenomenon [8,17,18].

The LRB consists of a laminate rubber bearing with a lead plug down its center as shown in Figure 3. The high lateral flexibility of the elastomer, working in shear, is the basis of the lateral displacement capacity. The lead plug, based on its perfect plastic deformation behavior, plays a role important to dissipate the generated energy for the bearing.

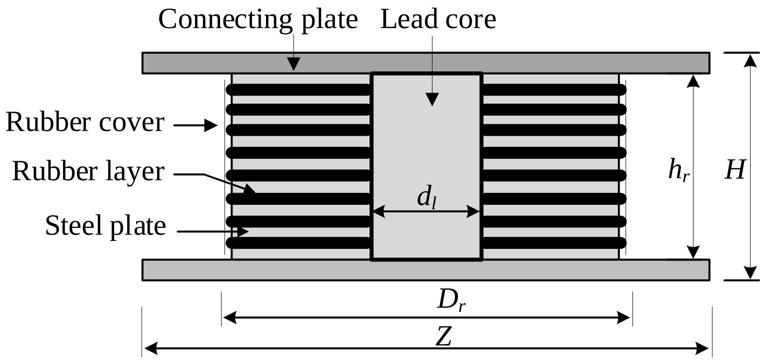

Figure 3. Structure of lead-rubber bearing isolator.

Generally, the LRB system provides high energy dissipation capacities with equivalent damping ratios up to 30% based on its practically perfect elastoplastic behavior in shear [1,17,19]. Further, the post-elastic stiffness of LRB is primarily contribution by the rubber component while its damping ratio can be modified easily by the selection of the appropriate size of the lead plug. Therefore, it can adapt extensively to different design requirements and considered as the ideal device for the SBI approach for buildings.

In moderate seismicity areas like Vietnam, although they have a relatively lower rate of earthquake activity and the damages by earthquake imparts may be less severe. Nevertheless, large earthquakes have occurred in these regions in the past and will inevitably occur in the future. Therefore, advanced earthquake design approaches are still needed to not only provide safety and extend the life of the construction but also to reduce maintenance costs after earthquakes [20,21].

Although the seismic base isolation design is mentioned in the Vietnamese code [5], its application in practice is still limited. This paper presents the effectiveness of LRB on the seismic responses of a typical multi-story building located in Hanoi, Vietnam.

The theoretical basis of the SBI for the building structure is first outlined by a simplified model of the isolated building structure. The bilinear model of SBI and the procedure of iteration are represented, which was considered as the simplified method, to determine the effective parameters of the equivalent linear viscoelastic model (i.e. effective stiffness and effective damping ratio) for isolator. Three-dimensional models of an 11-story building were analyzed to evaluate the effect of SBI on the seismic response of the structure. To do so, time history analysis was conducted with a record according to ground motion in Hanoi by using Etabs V17 software in combination with the Vietnamese code [5]. The effect of SBI was clarified by comparisons of the results between the fixed-base structure and isolated structure.

2. THEORETICAL BASIS OF SEISMIC ISOLATION

2.1. Linear theory of two-degree-of-freedom

Kelly [19] has given detailed the linear theory of seismic isolation base on the simplified structural model of a two-mass system as illustrated in Figure 4. The mass m represents the superstructure of the building and m_b is the mass of the base floor above the isolation systems. The structural properties are represented by k_s, c_s (stiffness and damping coefficient, respectively). Similarly, the isolation is characterized by k_b, c_b. Absolute displacements of the two masses are assumed by u_s and u_b. Accordingly, the relative displacements are used as defined below:

$$v_b = u_b - u_g;\; v_s = u_s - u_b, \tag{1}$$

where u_g is the ground displacement, v_b is the isolation system displacement and v_s is the inter-story drift.

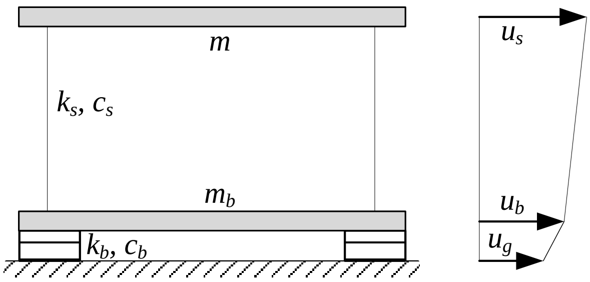

Figure 4. Simplified structural model of two·degrees-of-freedom isolated system.

The mathematical model of system is expressed in matrix form as follows:

$$\begin{bmatrix} M & m \\ m & m \end{bmatrix}\begin{Bmatrix} \ddot{v}_b \\ \ddot{v}_s \end{Bmatrix} + \begin{bmatrix} c_b & 0 \\ 0 & c_s \end{bmatrix}\begin{Bmatrix} \dot{v}_b \\ \dot{v}_s \end{Bmatrix} + \begin{bmatrix} k_b & 0 \\ 0 & k_s \end{bmatrix}\begin{Bmatrix} v_b \\ v_s \end{Bmatrix} = \begin{bmatrix} M & m \\ m & m \end{bmatrix}\begin{Bmatrix} 1 \\ 0 \end{Bmatrix}\ddot{u}_g, \tag{2}$$

where $M = m + m_b$. The form of equation (2) can be reduced as below:

$$\mathbf{M}\ddot{\mathbf{v}} + \mathbf{C}\dot{\mathbf{v}} + \mathbf{K}\mathbf{v} = -\mathbf{M}\mathbf{r}\ddot{u}_g. \tag{3}$$

The nominal frequencies ω_b and ω_s are determined as the following:

$$\omega_b^2 = \frac{k_b}{m + m_b}; \quad \omega_s^2 = \frac{k_s}{m}. \tag{4}$$

and the damping ratio ξ_b and ξ_s are given as the following:

$$2\omega_b\xi_b = \frac{c_b}{m + m_b}; \; 2\omega_s\xi_s = \frac{c_s}{m}. \tag{5}$$

2.2. Extension of theory to Multi-degree-of-freedom

The two-degree-of-freedom system of the equivalent linear model can be developed suitably for cases of a multi-story building. Generally, the structural system of the building is represented by a mass matrix, **M**, a damping matrix, **C**, and stiffness matrix, **K**. For the structure with fixed bases, the relative displacement, **u**, of mass that normalized to the ground can be given as:

$$\mathbf{M}\ddot{\mathbf{u}} + \mathbf{C}\dot{\mathbf{u}} + \mathbf{K}\mathbf{u} = -\mathbf{M}\mathbf{r}\ddot{u}_g, \tag{6}$$

where **r** is a vector that couples each degree of freedom to the ground motion.

For the isolated structural model, the base is characterized by mass m_b, the isolators are represented by the stiffness k_b, and damping c_b, equation (6) is becomes:

$$\mathbf{M}\ddot{\mathbf{v}} + \mathbf{C}\dot{\mathbf{v}} + \mathbf{K}\mathbf{v} = -\mathbf{M}\mathbf{r}\left(\ddot{u}_g + \ddot{v}_b\right), \tag{7}$$

where **v** and v_b are the displacement relative of the mass *m* to the base slab and the base slab relative to the ground, respectively. Then, the overall equation of motion for the global isolated structural model is:

$$\mathbf{r}^T\mathbf{M}\ddot{\mathbf{v}} + \left(m + m_b\right)\ddot{v}_b + c_b\dot{v}_b + k_b v_b = -\left(m + m_b\right)\ddot{u}_g. \tag{8}$$

In equation (8), the total mass of the building, *m*, is identified by $\mathbf{r}^T\mathbf{M}\mathbf{r}$, the total mass carried on the isolation system is calculated as $m + m_b$. These equations can be expressed in the following the matrix form:

$$\mathbf{M}^*\ddot{\mathbf{v}}^* + \mathbf{C}^*\dot{\mathbf{v}}^* + \mathbf{K}^*\mathbf{v}^* = -\mathbf{M}^*\mathbf{r}^*\ddot{u}_g, \tag{9}$$

where

$$\mathbf{M}^* = \begin{bmatrix} m + m_b & \mathbf{r}^T\mathbf{M} \\ \mathbf{M}\mathbf{r} & \mathbf{M} \end{bmatrix}; \quad \mathbf{C}^* = \begin{bmatrix} c_b & 0 \\ \mathbf{0} & \mathbf{C} \end{bmatrix}; \quad \mathbf{K}^* = \begin{bmatrix} k_b & 0 \\ \mathbf{0} & \mathbf{K} \end{bmatrix}; \quad \mathbf{r}^* = \begin{bmatrix} 1 \\ \mathbf{0} \end{bmatrix},$$

with

$$\mathbf{v}^* = \begin{bmatrix} v_b \\ \mathbf{v} \end{bmatrix}.$$

Equation (9) can be solved directly or through modal decomposition, numerical evaluation [14].

3. ESTIMATING PROPERTIES OF ISOLATOR BY EQUIVALENT BILINEAR MODEL

Practically, the isolation bearing can be modeled by an ideal bilinear model based on four main parameters such as: (i) the characteristic strength, *Q*; (ii) the post-yielding stiffness, K_2; (iii) yield displacement, D_y; and (iv) maximum displacement, D_{max}, as shown in Figure 5 [8].

The initial stiffness, K_1, and the effective stiffness, K_{eff}, of equivalent model can be determined as follows:

$$K_1 = \frac{Q}{D_y} + K_2; \tag{10}$$

$$K_{eff} = \frac{Q}{D_{\max}} + K_2, \tag{11}$$

where, the maximum displacement, D_{max}, can be determined from the spectral displacement given by the code as the following:

$$D_{\max} = \frac{MS_a\left(T_{eff}, \xi_{eff}\right)}{K_{eff}}, \tag{12}$$

where

$S_a(T)$ is the elastic response acceleration spectrum;
ξ_{eff} is the effective equivalent viscous damping ratio, expressed as a percentage;
T_{eff} is the effective period of the isolation system:

$$T_{eff} = 2\pi\sqrt{\frac{M}{K_{eff}}}, \tag{13}$$

The energy dissipated per cycle (EDC) is determined by the area under hysteresis loop and considered by an equivalent linear viscoelastic system:

$$W_D = EDC = 4Q\left(D_{\max} - D_y\right) = 2\pi\xi_{eff}K_{eff}D_{\max}^2. \tag{14}$$

Therefore, the effective equivalent damping ratio can be calculated as follows:

$$\xi_{eff} = \frac{4Q\left(D_{\max} - D_y\right)}{2\pi K_{eff} D_{\max}^2}. \tag{15}$$

Figure 5 illustrates a bilinear force-displacement relationship for a typical seismic isolation system that includes the characteristic parameters.

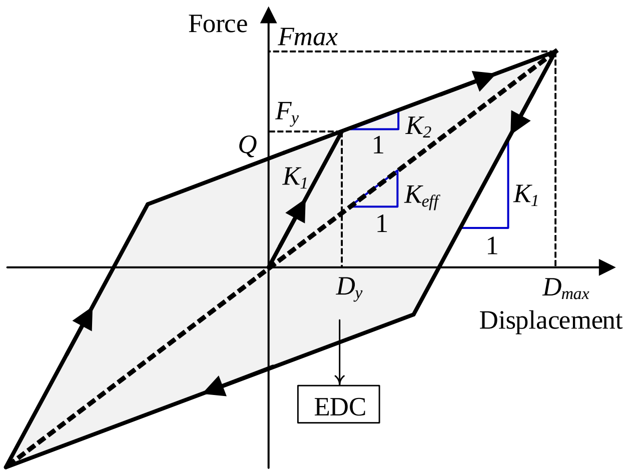

Figure 5. Parameters of bilinear model.

According to the bilinear model, three important parameters are derived:

$$Q = \frac{W_D}{4\left(D_{\max} - D_y\right)}; \tag{16}$$

$$K_2 = K_{eff} - \frac{Q}{D_{\max}}; \tag{17}$$

$$D_y = \frac{Q}{K_1 - K_2} = \frac{Q}{K_2\left(1/\alpha - 1\right)}, \tag{18}$$

where $\alpha = K_2/K_1$ is the post-elastic ratio.

According to the classification of Naeim and Kelly [8], certain SBI corresponds to a range of the post-elastic ratio, namely the lead-plug rubber bearing corresponding to α =[1/30÷1/15].

Because these equations are coupled with each other, it is necessary to use an iterative procedure to calculate the design parameters, which is clearly illustrated in Figure 6.

On focus to the application of LRB, it should be noted that the contribution of rubber component is significantly to the stiffness of bearing, meanwhile, its effects on the characteristic strength of the device (Q) (including the yield force, F_y) are relatively negligible when compared with the lead plug. Therefore, Q and F_y can be approximated only by the lead core as follows:

$$F_y = \frac{1}{\psi} f_{yL} \frac{\pi d_l^2}{4}; \tag{19}$$

$$Q = F_y\left(1-\alpha\right), \tag{20}$$

where f_{yL} is the shear yield stress of lead, d_l is the diameter of the lead plug, and ψ is load factor accounting for creep in lead (ψ =1 for seismic loads).

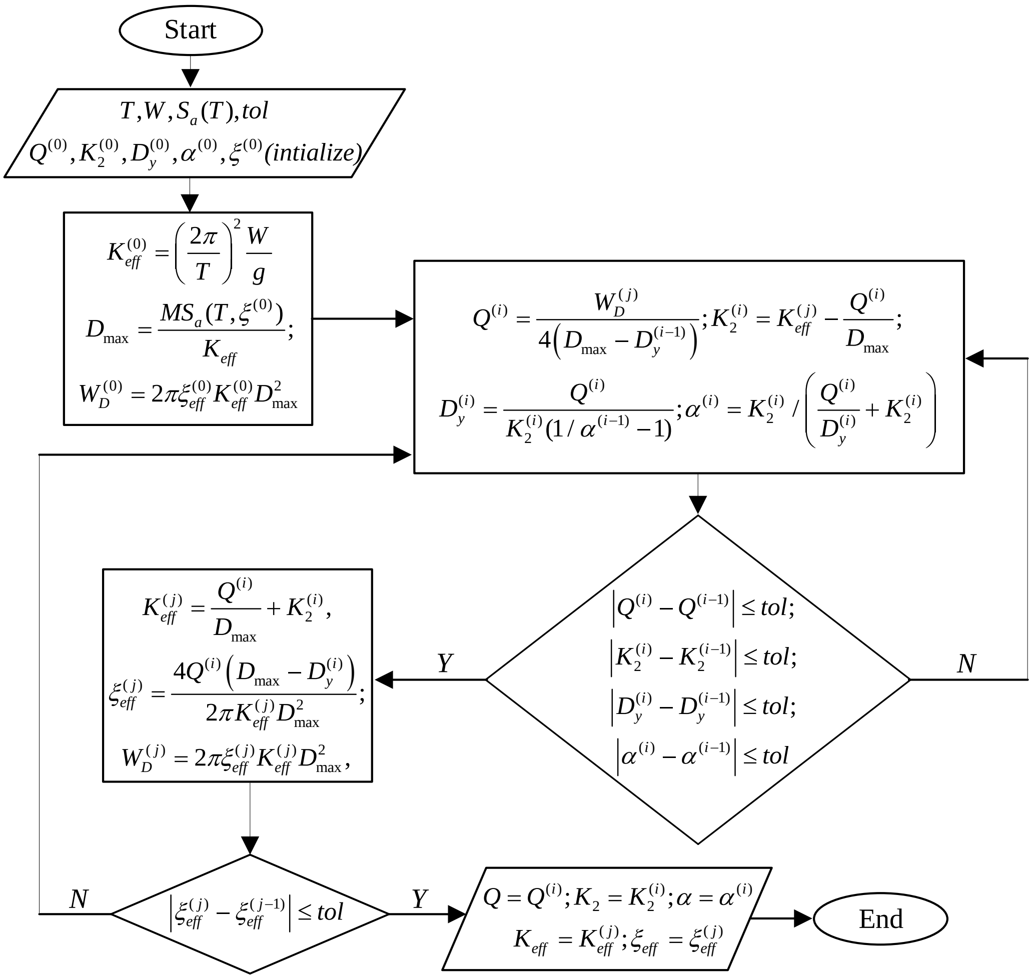

Figure 6. Iterative design procedure for determination of SBI properties.

4. BUILDING MODEL AND DESIGN

4.1 Model of building

Application on an office building with the properties of the model is detailed as below:

- Architecture: the sample model of building has 11 floors, including 1 basement and 10 stories. The floor height is 3.6m for the stories and 3.3m for the basement. The plan dimensions of the building are 27m x 24m, including 3 bays in the X and Y direction as shown in Figure 7.
- Structure: the beam dimensions are 30cm x 70cm for the main beam systems, sub-beam are 25cm x 50cm; the cross-section dimensions of columns: from 1st to 4th story 80cm x 80cm; from 5th to 8th story 70cm x 70cm; from 9th to the roof 60cm x 60cm; The concrete wall thickness is 25cm; and the floor thickness is 15cm.
- Material: concrete grade #B30, reinforced grade CB400-V.
- Loading: the floor loading: dead load 150 daN/m2, live load 240 daN/m2 (on the floor) and 90 daN/m2 (on the roof); the building is located in Hanoi, based on soil type C and subjected to acceleration with a_g = 0.1032g and the behaviour factor, q=3.9 [5].

Figure 7 shows the 3D model of the building by using Etabs [22].

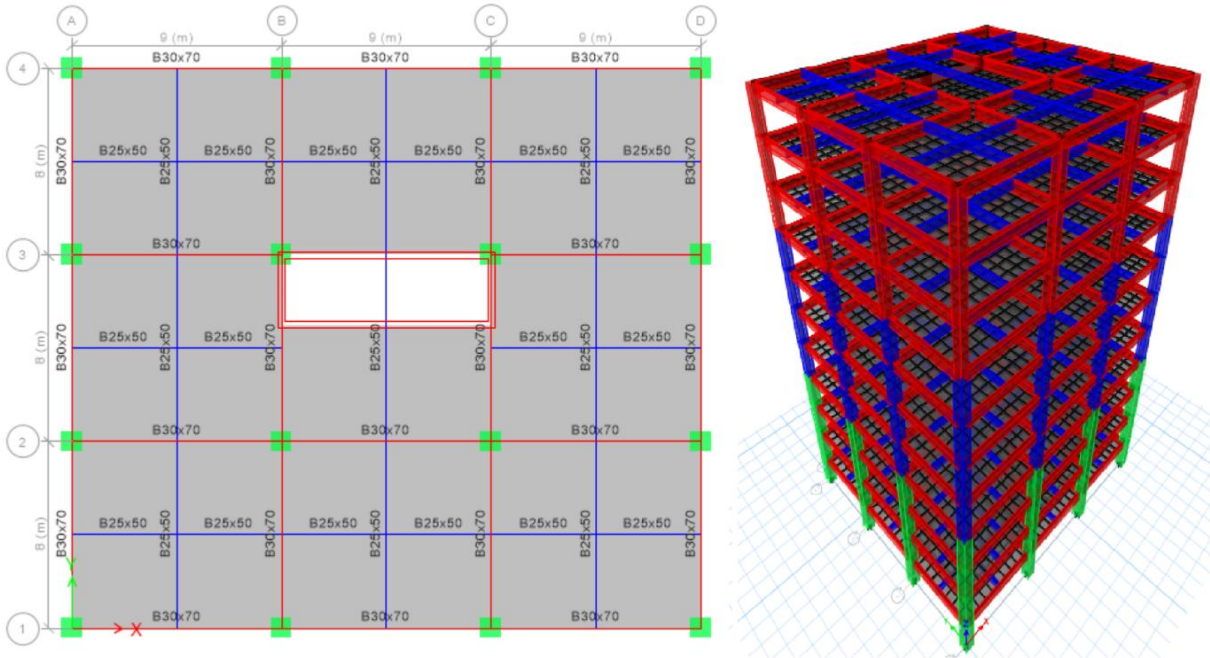

Figure 7. Specific floor plan and 3D model of the building.

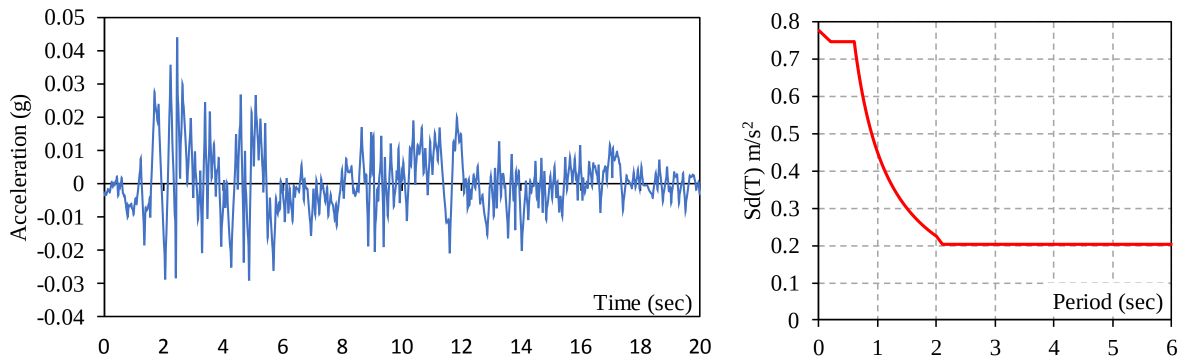

Figure 8. Spectrally acceleration time history and horizontal design spectrum used for study.

4.2 Determination isolators' properties

The total mass of building is M=7023000 (kg) used to estimate the parameters of the isolator. Assume that the damping ratio of isolator $\xi_{eff} = 20\%$, corresponding to interesting value of lead plug rubber bearing, [8]; the effective period of the fundamental mode of isolated building is assumed that T_{eff} = 2.5(s); $\alpha = 0.05$ ($\alpha = 1/30 \div 1/15$ for LRB). Based on the block diagram in Figure 6, the properties of a single equivalent isolator are obtained as: yield force, Q= 1753 kN; pre-yield stiffness, K_2= 30085 kN/m; effective stiffness, K_{eff}= 44361 kN/m, D_{max}= 0.123 m; dy=0.0029 m.

The required area of pads is approximately equal: A_r=7023x9.81x1.35/10^4=9.30 m^2, selecting 19 lead plug rubber bearings with the diameter of 800mm in the bottom of the columns and the concrete walls, so that A_r=9.55 m^2.

The thickness of elastomer to fit with the total effective stiffness: h_r=GA/K_{eff}=10^3x9.55/44361=0.215 m. Selecting the bearing with 10 layers of 16 mm, the shims are 2mm each and the end plates are 25mm, so that the total height is 0.228 m.

The yield strength of lead is taken as 10 MPa, so that the total area of lead plug needed is: A_l= Q/0.95/10^4=0.185 m^2. Choosing the lead plug with the diameter of 120 mm, then the total area of the lead plug is A_l = 19xπx0.120^2/4 = 0.215 m^2, F_y=2150 kN and Q=F_yx(1-0.05)=2042 kN.

Lead-plug bearings are usually from a low-damping, high-strength rubber with a modulus at 100% shear strain that might vary from 0.4 to 0.7 MPa [8,17]. The shear modulus value of lead is assumed equal to 0.6 MPa. Then, the post-yield stiffness of plain elastomeric bearings is given by:

$$K_2 = \frac{G(A_b - A_l)}{h} = \frac{0.6x10^3\left(9.55 - 0.215\right)}{0.228} = 24566\,kN/m.$$

The total effective stiffness K_{eff} is given as follows:

$$K_{eff} = 24566 + \frac{2042}{0.123} = 41171 kN/m.$$

and $W_D = 4x2042x(0.123 - 0.0029) = 981 kN/m$; $\xi_{eff} = 981/(2\pi x 41171 x 0.123^2) = 25{,}1\%$.

The total effective damping coefficient C_{eff} is given as:

$$C_{eff} = 2\xi_{eff}\sqrt{K_{eff}M} = 8526\,kNs/m.$$

The total initial stiffness K_1 is given as:

$$K_1 = K_2/\alpha = 491316\,kN/m.$$

Accordingly, Table 1 shows the properties for one of 19 similar systems used for the building.

Table 1. Properties of a single SBI.

M (kg)	W (kN)	K_{eff} (kN/m)	C_{eff} (kNs/m)	K_1 (kN/m)	Q (kN)	α
370000	3626	2167	449	25859	107	0.05

4.3 Modeling and results

The link elements are employed to modeling SBI in Etabs software with the property data as shown in Table 1. Both models of the fixed-base building structure and the isolated-base building structure are conducted by time history analyses with an artificial ground motion and spectral acceleration, which was built accordingly to TCVN 9386: 2012 by using Etabs, as shown in Figure 8. The seismic performance of SBI is primarily considered overall based on the reduction of shear force at the base of the building structure and the drift at the floors. The results are taken into comparing in order to evaluate the effectiveness of SBI as shown in Figures 9-15.

Figure 9 shows the period value of the first five modes of vibration. Accordingly, the SBI application produces a significant effect on the vibration modes, especially on the fundamental mode. Namely, for isolated building, the period of the first two modes of vibration is extended significantly when compared to the fixed-base building structure. The difference of the fundamental period between the analysis result and the value taken in the simplified procedure is considered as the consequence of multi-degrees of freedom in the three-dimensional analysis model.

In general, the seismically isolated structure will be interested in the first modes of vibration, which contribute mostly to structural dynamic responses. In this study, the first modes of vibration are used to investigate the SBI efficacy. Correspondingly, Figure 10 shows the first three modes of vibration of the building. The results illustrate that for the isolated building, the deformation occurs mainly in SBI rather than structural components in the fixed-base structure. Moreover, the effect of bending due to the seismic force is greatly reduced in the isolated building when compared with the fixed-base building.

Figure 11 shows the story drift diagram of the buildings. A significant reduction of drift is gotten by using SBI, especially at the top of the building.

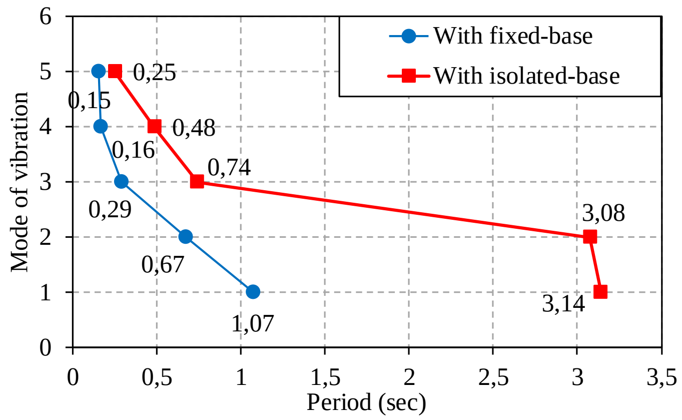

Figure 9. Model periods of structures' vibration.

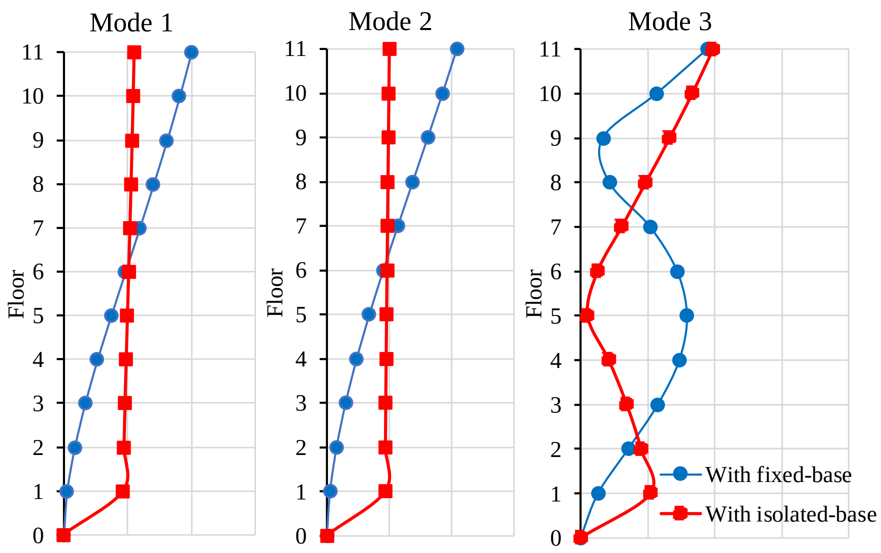

Figure 10. Modal shapes analysis.

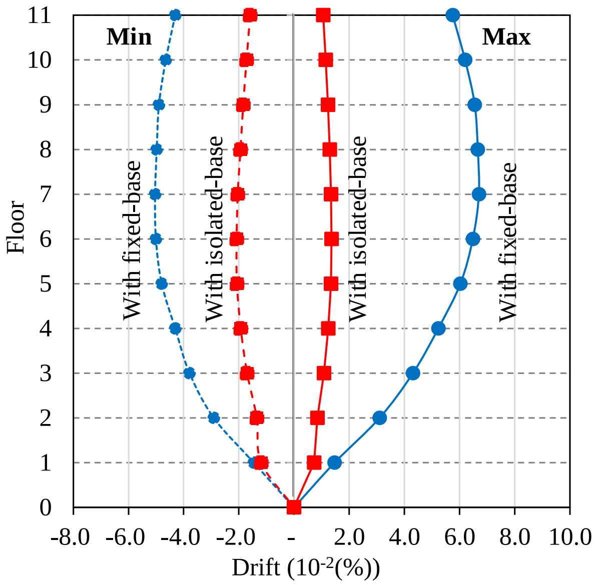

Figure 11. Story drift diagram of building subjected to seismic action in Y direction.

Figure 12 to Figure 15 show the comparisons of time history responses for two models in terms of the base shear force, acceleration at the top floor, the displacement at the top floor, which are the parameters that most clearly show the effects of SBI.

Figure 12 and Figure 13 clearly demonstrate that the base shear force at the base and the acceleration at the top floor of the isolated building are significantly reduced when compared with the fixed-base building, suggesting that the seismic performance of the structural building is significantly increased by using SBI. In other words, the application of SBI considerably reduces the requirement for the demand of structural seismic resistances.

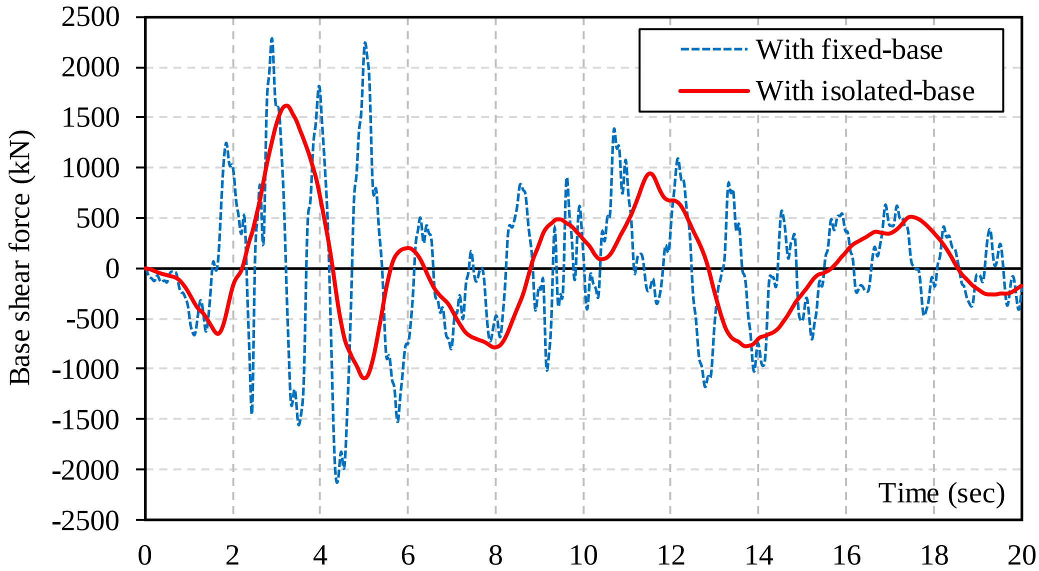

Figure 12. Dynamic base shear force in Y direction.

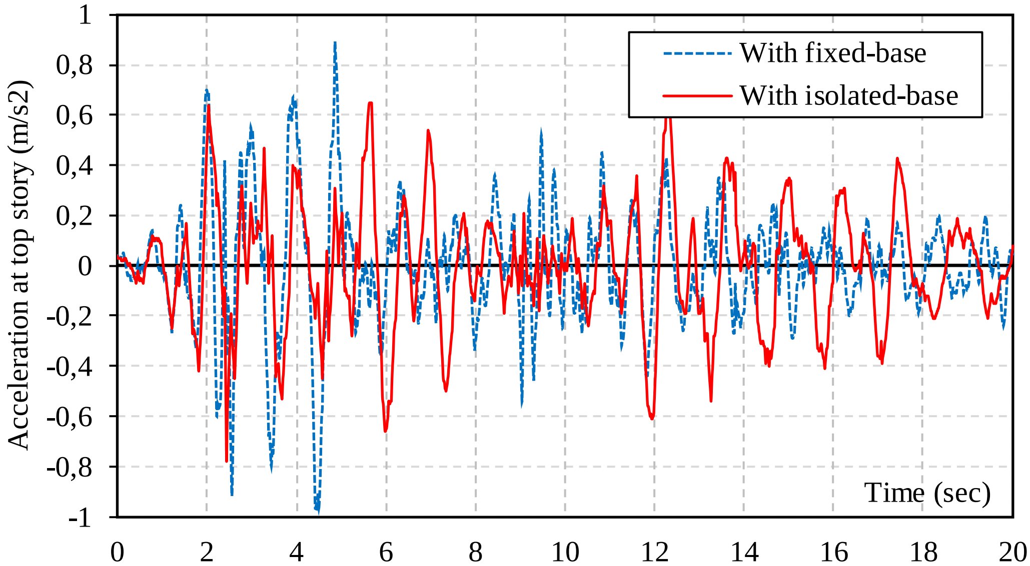

Figure 13. Dynamic acceleration at the top story.

Figure 14 shows a comparison of the absolute displacement at the top floor between the fixed-base building and the isolated building. The absolute displacement in the isolated building is significantly higher than the fixed-base building. However, this displacement occurs primarily in the isolator, rather than in the structural components, as illustrated in Figure 15. Accordingly, the relative displacement of structure in the isolated building is much lower than the fixed-base building. Therefore, the verification of the stability of the building after the earthquake just focuses only on the location of isolators.

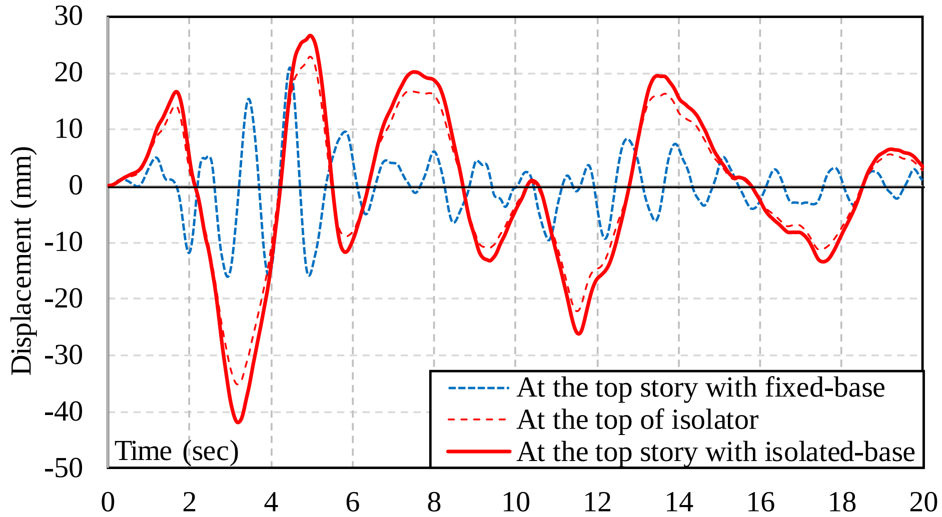

Figure 14. Dynamic absolute displacement at the top story (column 1B) in Y direction.

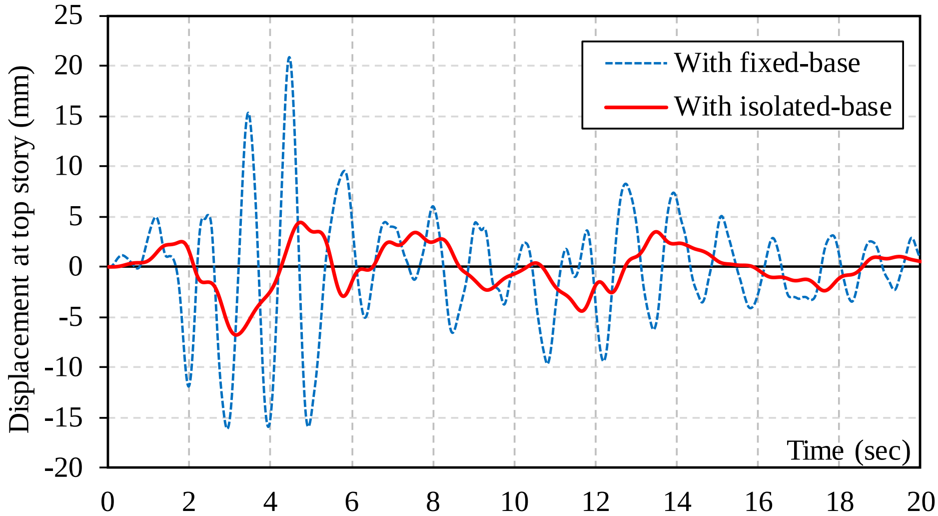

Figure 15. Dynamic relative displacement at the top story (column 1B) in Y direction.

The effectiveness of SBI application is resumed in detail in Table 2. Accordingly, the base shear forces reduce from 36% up to 56%, the acceleration at the top floor reduces around 58%, while the displacement at the top of building reduces from 58% to 79% by using the isolator.

Table 2. Comparison between fixed-base and isolated-base structure.

Ord	Content	Max value			Min value		
		FB (1)	IB (2)	Ratios (1)/(2), %	FB (3)	IB (4)	Ratios (3)/(4), %
1	Base shear force (Y), kN	2.276,4	1.443,8	36,5	-2.134,2	-941,0	55,9
2	Absolute displacement at the top story (Y), mm	20,9	26,5	-26,8	-16,1	-41,9	-61,6
3	Relative displacement at the top strory (Y), mm	20,9	4,4	78,8	-16,1	-6,79	57,8
4	Acceleration at the top strory (Y), m/s2	0,89	0,37	58,43	-0,98	-0,40	59,18

5. CONCLUSIONS

In this paper, the effects of SBI on seismic responses of the multi-story building have been performed. The simplified method for estimating the properties of lead-plug rubber bearing was conducted based on the iterative procedure by using the equivalent bilinear model. The seismic performance of LRB was investigated through the numerical analyses of an 11-story building. The obtained results show that SBI strongly affects the vibration of the building. It allows to extend the period of the fundamental mode, therefore, reduces the impact of the ground motion on the structure. Further, in the isolated structure, the deformation due to the effect of earthquakes occurs mainly in the SBI instead of structural components as in the fixed-base building structure, resulting in a significant reduction of the internal force and displacement of the main structure's response. Therefore, the seismic resistance of the building is greatly improved. It also confirms the feasibility of the SBI application for multi-story building structures in the moderate seismic regions such as Vietnam.

REFERENCES

[1]. AASHTO 2014 *Guide Specifications for Seismic Isolation Design* (Washington, DC)
[2]. ASCE 41-06 2006 *Seismic Rehabilitation of Existing Buildings, American Society of Civil*

Engineers (Reston, Virginia)
[3]. CNBC 2016 *Canadian National Building Code*
[4]. EN 1998-1 2005 *Eurocode 8 : Design of structures for earthquake resistance. Part 1: General rules, seismic actions and rules for buildings* vol 1 (CEN)
[5]. TCVN 9386 2012 *Design of structures for earthquake resistances, Part 1* (Ha Noi, Viet Nam)
[6]. Aiqun Li 2020 *Vibration Control for Building Structures: Theory and Application* (Springer)
[7]. Mansouri S and Nazari A 2017 The effects of using different seismic bearing on the behavior and seismic response of high-rise building *Civil Engineering Journal* **3** 160–71
[8]. Naeim F and Kelly J M 1999 *Design of Seismic Isolated Structures: From Theory to Practice* (John Wiley & Sons, INC)
[9]. Sahu G and Sahu P 2019 Comparative Analysis of Effects of Base Isolator & Fluid Viscous Damper on Response of a RCC Structure *International Research Journal of Engineering and Technology* **6** 94–101
[10]. Shevale S S, Kadam S S, Pise C P, Pawar Y P, Deshmukh C M and Mohite D D 2016 Seismic behaviour of multi-storied building by using tuned mass damper and base isolation : A Review *Journal of Engineering Research and Application* **6** 1–6
[11]. Bozorgnia Y 2004 *Earthquake Engineering: From Engineering Seismology to Performance-Based Engineering* (CRC Press)
[12]. Datta T K 2010 *Seismic analysis of structures* (John Wiley & Sons.)
[13]. Bisch P, Carvalho E, Degee H, Fajfar P, Fardis M, Franchin P, Kreslin M, Pecker A, Pinto P, Plumier A, Somja H and Tsionis G 2012 *Eurocode 8: Seismic Design of Buildings Worked examples* (Publications Office of the European Union)
[14]. Chopra A K 2017 *Dynamics of structures. theory and applications to earthquake engineering* (Prentice Hall)
[15]. Morgan T A and Mahin S A 2011 The use of base isolation systems to achieve complex seismic performance objectives *Pacific Earthquake Engineering Research Center*
[16]. Buckle I G, Constantinou M C, Diceli M and Ghasemi H 2006 *Seismic isolation of highway bridges* (Federal Highway Administration)
[17]. EN 1337-3 2005 *Structural Bearings - Part 3: Elastomeric bearings* (CEN)
[18]. Constantinou M C, Tsopelas P, Kasalanati A and Wolff E D 1999 *Property modification factors for seismic isolation bearings* (Multidisciplinary Center for Earthquake Engineering Research)
[19]. Kelly J M 1993 *Earthquake Resistant Design with Rubber* (Springer-Verlag)
[20]. Chen Y F 2004 Assessment of the current US seismic displacement requirements for bridges in a low–moderate seismic zone *Engineering Structures* **26** 1365-1379.
[21]. Nordenson, G. J. and Bell G R 2000 Seismic design requirements for regions of moderate seismicity *Earthquake Spectra* **16** 205-225.
[22]. CSI 2018 Etabs V17.0.1